Todo list

OBSERVATIONS OF PWNE WITH THE FERMI GAMMA-RAY SPACE TELESCOPE

A DISSERTATION
SUBMITTED TO THE DEPARTMENT OF PHYSICS
AND THE COMMITTEE ON GRADUATE STUDIES
OF STANFORD UNIVERSITY
IN PARTIAL FULFILLMENT OF THE REQUIREMENTS
FOR THE DEGREE OF
DOCTOR OF PHILOSOPHY

Joshua Jeremy Lande

January 2013

I certify that I have read this dissertation and that, in my opinion, it is fully adequate in scope and quality as a dissertation for the degree of Doctor of Philosophy.

(Stefan Funk) Principal Adviser

I certify that I have read this dissertation and that, in my opinion, it is fully adequate in scope and quality as a dissertation for the degree of Doctor of Philosophy.

(Elliott Bloom)

I certify that I have read this dissertation and that, in my opinion, it is fully adequate in scope and quality as a dissertation for the degree of Doctor of Philosophy.

(Roger Romani)

Approved for the University Committee on Graduate Studies

Abstract

Two things fill the mind with ever-increasing wonder and awe, the more often and the more intensely the mind of thought is drawn to them: the starry heavens above me and the moral law within me." – Immanuel Kant

The launch of the *Fermi* Gamma-ray space telescope in 2008 offered an unprecedented view into the γ-ray sky.

All the things we can learn with the Large Area Telescope (LAT)

Development of a new analysis method for studying spatially-extended Pulsar Wind Nebulae (PWNe) using `pointlike`.

A monte-carlo validation of the analysis method.

Search for new spatially-extended sources with the LAT.

Observations of PWNe in the off-peak region of LAT detected pulsars.

Search for PWNe counterparts to TeV sources.

Using the population of PWNe to understand the radiation mechanism of PWNe.

Acknowledgement

Acknowkege the educational institutes which taught me physics: My high school HB Woodlawn, my undergraduate institution Marlboro College, and my Stanford University.

First, I would like to acknowlege those mentors who inspired me to get a PhD.

- Mark Dodge, my high school physics teacher.
- Ron Turner, my internship adviser at Analytic Services (ANSER) during the GWU Science and Engineering Apprentice Program (SEAP)
- Anthony Tyson at UC Davis for my SULI Internship
- Apurva Mehta and Sam Webb sam Web at SLAC SULI Internship.

During my PhD I was helped by an almost overwhelminlgy large number of people in the LAT collaboration.

People at Stanford/SLAC: Stefan Funk, Elliott Bloom, Markus Ackermann, Tobias Jogler, Junichiro Katsuta, Yasunobu Uchiyama, Seth Digel, James Chiang

`pointlike` collaborators: Matthew Kerr, Toby Burnett, Eric Wallace, Marshall Roth

Pulsar Collaborators: David Smith, Matthew Kerr, Peter den Hartog, Tyrel Johnson, Damien Parent, Ozlem Celik

Careful review of text: Jean Ballet, Johann Cohen-Tanugi

I would like to thank the PWNe people Thank the people in Bordeaux: Marianne Lemoine-Goumard, Romain Rousseau, and Marie-Hélène Grondin

Fermi SLAC Grad Students: Keith Bechtol, Alex Drlica-Wagner, Alice Allafort, Herman Lee Yvonne Edmonds, Bijan Berenji, Ping Wang, Warit Mitthumsiri

Additional Astro Stanford Graduate Students: Helen Craig, Michael Shaw, Adam Van Etten, Kyle Watters

Additonal Graduate Students at Stanford: Dan Riley, Joel Frederico, Ahmed Ismail, Joshua Cogan, Kunal Sahasrabuddhe,

Contents

List of Tables

List of Figures

List of Acronyms

The following acronyms are used in this text, and are included here for reference:

SA Solid Angle

LAT Large Area Telescope

PWN Pulsar Wind Nebula

IC Inverse Compoton

2CG The Second COS-B catalog

2FGL The Second *Fermi*-LAT catalog

CGS The Centimetre-Gram-Second System of Units

PL power law

ECPL exponentially-cutoff power law

BPL broken-power law

MIT Massachusetts Institute of Technology

OSO-3 the Third Orbiting Solar Observatory

SAS-2 the second Small Astronomy Satellite

EGRET the Energetic Gamma Ray Experiment Telescope

CGRO the Compton Gamma Ray Observatory

ESA the European Space Agency

NASA the National Aeronautics and Space Administration

Chapter 1

Overview

In Chapter 2, we discuss the history of γ-ray astrophysics, ...

Chapter 2

Gamma-ray Astrophysics

2.1 The History of Gamma-ray Astrophysics

Astronomy has historically been almost entirely concerned with studying the photons that arrive from outer space. Because of their charge neutrality, photons are not defected by intergalactic electric and magnetic fields and therefore point back to the objects emitting them. Historically, the field of astronomy concerned the study of visible light. Slowly, over time, astronomers expanded their view across the electromagnetic spectrum.

Infrared radiation from the sun was first observed by William Herschel in 1980 (Herschel 1800). The first extraterrestrial source of radio waves was detected by Jansky in 1933 (Jansky 1933).

The development of rockets and sattelites in the 20th ceuntry allowed the field of astronomy to expand futher, allowering observations at wavelengths that would otherwise be absorbed in the atmosphere. The first ultraviolet observation of the sun was performed in 1946 from a captured V-2 rocket (Baum et al. 1946). Observations of solar x-rays were also first carried out on a captured V-2 Rocket in 1949 (Burnight 1949)

It was only natural to wonder about the universe at even higher energies. As is common in the field of physics, the prediction of the detection of cosmic γ-rays far proceded their discovery. Feenberg & Primakoff (1948) theorized that the interaction

of starlight with cosmic rays could produce γ-rays through Inverse Compoton (IC) upscattering. Following the discovery of the neutral pion in 1949, Hayakawa (1952) predicted that γ-ray emission could be observed from the decay of neutral pions when cosmic rays interacted with interstellar matter. And in the same year, Hutchinson (1952) discussed the bremsstrahlung radiation of cosmic-ray electrons. Morrison (1958) first predicted the detection of several sources of γ-rays including solar flares, Pulsar Wind Nebulae (PWNe), and active galaxies.

Why Gamma-rays can't make it to the ground

Discuss Balloon gamma-ray detectors. See discussion on p859 (comparison with other experiments) of Kraushaar et al 1965. What was the background from, earth albedo gammas I think? See also Kraushaar et al 1972 p342's discussion of the balloon experiments: Hulsizer and Rossi (1949), ... See also William Tomkin's section 2.2.1 on Balloon experiments (page 8) for references to galactic plane emission being measured by balloon experiments in 1970.

Attempts were made in the 1940s and 1950s to determine the composition of cosmic rays using balloon-based experiments. See, for example Critchfield et al. (1952) and Hulsizer & Rossi (1948). But the attempt to observe cosmic γ-rays was hampered by the strong background of atmospheric albedo γ-rays.

The first space-based γ-ray detector was Explorer XI Kraushaar et al. (1965). It was developed at Massachusetts Institute of Technology (MIT) under the direction of William L. Kraushaar. It employed a sandwich scintillator and a Cherenkov counter to direct the position and energy of incoming γ-rays and was surounded by a plastic anticoincidence scintilation counter. The sandwich detector had an area of $\sim 45\text{cm}^2$, but an effective area of only $\sim 7\text{cm}^2$, corresonding to a detector efficiency of $\sim 15\%$.

What was the energy range of explorer ii

It was launched on boad Explorer XI on April 27, 1961. The instrument was in opreation for 7 months, but only 141 hours of data were of acceptable quality. Using these observations, Explorer XI observed 31 γ-rays and, because the distribution a distribution of these γ-rays was consistent with being isotropic, the experiment could not firmly identify the γ-rays as being cosmic in nature.

Describe scintilation detector better. Read William Tomkin's thesis, page 8.

The first definitive detection of γ-ray came in 1962 by an experiment on the Ranger 3 moon probe (Arnold et al. 1962). It detected an isotropic flux of γ-rays in the 0.5 MeV to 2.1 MeV energy range.

the Third Orbiting Solar Observatory (OSO-3), also developed by Kraushaar, followed Explorer XI as the next major astrophysical γ-ray detector Kraushaar et al. (1972). The OSO-3 sattelite allowed the on board γ-ray detected to have an improved weight, power, telemetry, and expsoure, creating a more sensitive experiment. The experiment operated in the energy range from 50 MeV to $\sim$ 400 MeV and had an effective area ~ 9 cm^2.

It was launched on March 8, 1967 and operated for 16 months, measuring 621 cosmic γ-rays. The most important result of the expirment was to measure a strong anisotrophy in the distribution of the γ-rays with a strong clustering of γ-rays towards the Galactic plane. Figure 2.1 shows a skymap of these γ-rays. This experiment confirmed both a Galactic component to the γ-ray sky as well as an additional isotropic component, hypothesised to be extragalactic in origin.

What was the PSF of OSO-3? could it be pointed?

Concurently with the major adavnces in space-based γ-ray detects came improved balloon-based γ-ray detectors.

Discuss Kniffen & Fichtel (1970) and Browning et al. (1971). Do a literature seach to see if there are other balloon experiments which detected similar stuff.

The next major advancement in γ-ray astronomy came from the the second Small Astronomy Satellite (SAS-2) and COS-B missions.

SAS-2 was a dedicated γ-ray detector launched by the National Aeronautics and Space Administration (NASA) in November 15, 1972. SAS-2 was Fichtel et al. (1975) It improved upon OSO-3 by incorporating a spark chamber and having an overall larger size. The size of the active area of the detector was 640 cm^2 and the experiment had a much improved effective area of $\sim 115\, cm^2$. The spark chamber allowed for a seperate measurement of the electron and positron tracks, which allowd for improved directional reconstruction of the incident γ-ray. SAS-2 had a PSF $\sim 5^\circ$ at 30 MeV

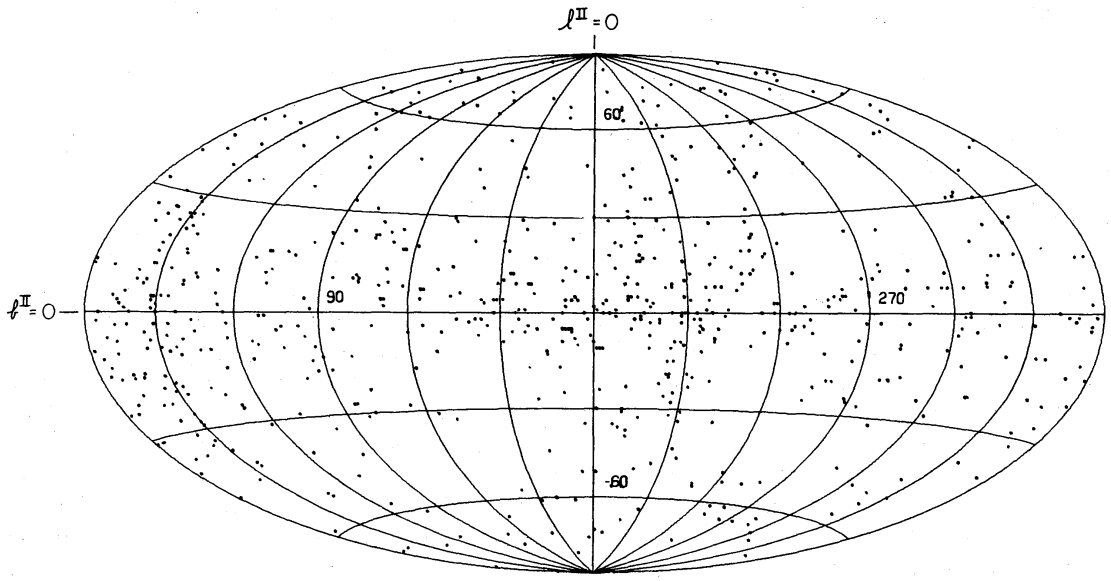

Figure 2.1: The position of all 621 cosmic γ-rays detected by OSO-3. This figure is from Kraushaar et al. (1972).

and $\sim 1^{\circ}$ at 1 GeV.

SAS-2 collected data for over 6 months before a power supply failure ended data collection. SAS-2 Observed over 8,000 γ-ray photons covering $\sim$ 55% of the sky including most of the Galactic plane. SAS-2 disovered strong emission along the Galactic plane and particularly towards the Galactic cente. It also discovered pulsations from the Crab (Fichtel et al. 1975) and Vela pulsar (Thompson et al. 1977b). In addition, SAS-2 discovered Geminga, the first γ-ray source with no compelling multiwavelenth counterpart (Thompson et al. 1977a). Gemina was eventually discovered to be a pulsar by the Energetic Gamma Ray Experiment Telescope (EGRET) (Bertsch et al. 1992) and retroactivly by SAS-2 (Mattox et al. 1992).

on August 9, 1975, the European Space Agency (ESA) launched COS-B, a γ-ray detector similar to SAS-2. COS-B included a spark chamber but improved upon the design of SAS-2 by including a calorimiter below the spark chamber which improved the energy resolution to $< 100\%$ for energies $\sim 3\,\mathrm{GeV}$ (Bignami et al. 1975). COS-B has a comparable effective area to SAS-2: $\sim 50\,\mathrm{cm}^2$ at $\sim 400\,\mathrm{MeV}$ (Bignami et al.

1975).

Over what energy range did COS-B observe photons?

COS-B operated successfully for over 6 years and produced the first detailed catalog of the γ-ray sky. In total, COS-B observed $\sim 80,000$ photons **?**. The Second COS-B catalog (2CG) detailed the detection 25 γ-ray sources for $E > 100\,\mathrm{MeV}$ (Swanenburg et al. 1981). Figure 2.1 shows a map of these sources. Of these sources, the vast majority lay along the galactic plane and could not be positivly identified with sources observed at other wavelenths. In addition, COS-B observed the first ever extragalactic γ-ray source, (3C273, Swanenburg et al. 1978).

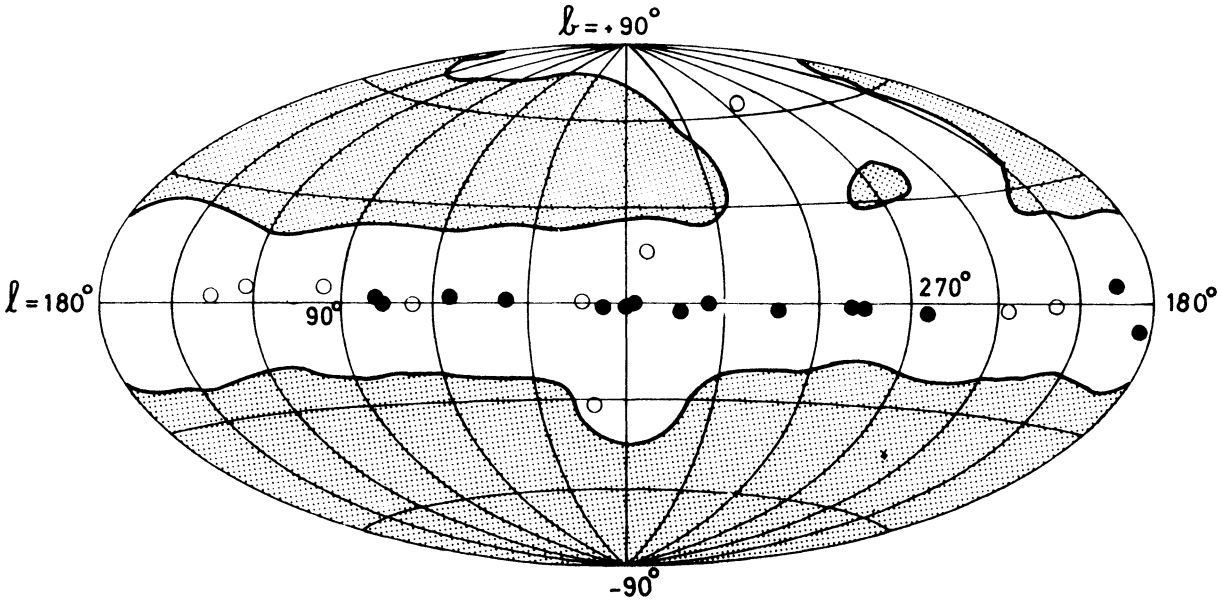

Figure 2.2: A map of the sources observed by COS-B. The filled circles represent brighter sources. The unshaded region corresponds to the parts of the sky observed by COS-B. This figure is from Swanenburg et al. (1981).

EGRET on board the Compton Gamma Ray Observatory (CGRO)

Figure out of EGRET was first to detect a PWNe (crab nebula. EGRET analysis: `http://adsabs.harvard.edu/abs/1993ApJ...409..697N` COS-B Analysis: `http://adsabs.harvard.edu/abs/1987A%26A...174...85C`

How many γ-rays EGRET detect?

How many pulsars did EGRET detect?

- AGILE
- *Fermi*
- Short description of the history of TeV astronomy

2.2 Astrophysical Sources of Gamma-ray

2.2.1 Pulsars

Describe pulsar physics. See description from Carroll and Ostlie page 593

$$\dot{E} = 4\pi^2 I \dot{P}/P \tag{2.1}$$

$$\tau_c = P/2\dot{P} \tag{2.2}$$

2.2.2 Pulsar Wind Nebulae

2.2.3 Supernova Remenants

2.3 The *Fermi* Gamma-ray Space Telescope

2.4 Radiation Processes in Gamma-ray Astrophysics

- The non-thermal radiation processes typical in astrophysics are most comonly

2.4.1 Synchrotron

2.4.2 Inverse Compoton

IC emission is ...

2.4.3 Bremsstrahlung

2.4.4 Pi0 Decay

2.5 Modeling the Galactic Diffuse and Isotropic Gamma-ray Background

Include discussion of modeling, if time permitting

- Discuss the historical Observations of galactic diffuse emission

  Mention how OSO-3 first detected the *gamma*-rays from the galaxy: Section 2.1.

- GALPROP model of diffuse emission. Reference: `http://arxiv.org/abs/1202.4039`
- Emperical Ring model of galactic diffuse emisson.
- The isotropic background: `http://arxiv.org/abs/1002.3603`
- Galactic diffuse emission is primarily composed of ...
- Something about how great galprop is.
- Something about

2.6 Sources Detected by the Fermi LAT

- A variety of sources detected by the LAT:

2.6.1 The Second *Fermi*-LAT catalog (2FGL)

2FGL was a catalog by the LAT collaboration containing XXX Sources.

Describe Catalog

- Citation is Nolan et al. (2012)
- Source classification method
- Number of sources detected by the Large Area Telescope (LAT)
- Forward reference Chapter 3, which does a more thorough description of likelihood analysis method.
- Source classes/associations

2.6.2 The Second Fermi Pulsar Catalog

- Process of detecting Pulsars with the LAT
- Number of pulsars detected by the LAT

2.6.3 PWNe Detected by the LAT

Crab

Vela X

MSH 15-52

HESS J1825

HESS J1857

2FGL J1857 + 026

1. Reference is Rousseau et al. (2012)
2. `http://arxiv.org/pdf/1206.3324v1.pdf`

Chapter 3

Maximum-likelihood analysis of LAT data

In this chapter, we discuss maximum-likelihood analysis, the principle analysis method used to perform spectral and spatial analysis of LAT data. In Section 3.1, we discuss the reasons necessary for employing this analysis procedure compared to other simpler analysis methods. In Section 3.2, we describe the benefits of a maximum-likelihood analysis. In Section 3.3, we discuss the steps invovled in defining a complete model of the sky, a necessary part of any likelihood analysis.

In Section 3.5, we discuss the standard implementation of binned maximum likelihood in the LAT Science Tools and in particular the tool `gtlike`. In Section 3.6, we then discuss the `pointlike` pacakge, an alterate package for maximum-likelihood analysis of LAT data. We discuss the similarities and differences between `pointlike` and `gtlike`.

In the next chapter (Chapter 4), we will discuss the addition of capability into `pointlike` for studying spatially-extended sources and the analysis method which will be used in this paper to study spatially-extended sources.

We not that much of the notation and formulation of likelihood analysis in this chapter follows Kerr (2010).

3.1 Motivations for Maximum-Likelihood Analysis of Gamma-ray Data

Traditonally, spectral and spatial analysis of astrophysical data relies on a process known as aperture photometry. In this process, a source in the data is analyzed by directly measuring the number of photons coming from the object. This process is done by measuring the counts within a given radius of the source and subtracting from it a background level estimated from a nearby region. Often, the source's flux is calibrated by measurements of nearby objects with known fluxes. Otherwise, the flux can be obtained from by dividing the number of counts from the source by the telesocpe's size, the observation time, and the telescope's conversion efficiency.

Similarly, for faint sources the statistical significance of the detection can be obtained from the Poission nature of the data. For TeV experiments such as H.E.S.S., this analysis method is described in Li & Ma (1983).

Unfortunately, this simpler analysis method is inadequate for dealing with the complexities introduced in analyzing LAT data.

Most importantly, aperture photometry assumed that the background is istropic so that the background level below the source can be estimated from nearby regions. As was discussed in Section 2.5, the Galactic diffuse emission is highly anistropic, rendering this assumption invalid.

In addition, this method is not optimal due to the high density of sources detected in the Gamma-ray sky. 2FGL reported on the detection of 1873 sources, which corresponds to an average source spacing of $\sim 5^\circ$. But within the inner 45° of the galactic plane in longitude and 0.5° of the galactic plane in latitidue, there are 73 sources, corresponding to a source density of ~ 1 source per square degree. The aperature photometry method is unable to effecitvly fit multiple sources when the tails of the PSF overlap and furthermore make background estimation problematic.

Finally, this method is suboptimal due to the large energy range of LAT observations. A typical spectral analysis studies a source from an energy of 100 MeV to energies above 100 GeV. Similarly, as was shown in , the PSF of the LAT is rather broad ($\gtrsim 1^\circ$) at low energy and much narrower ($\sim 0.1^\circ$) at higher energies. Therefore,

what section discusses energy

there is a much higher sensitivty to the higher energy photons coming from a source. But simple aperture photometry method would ignore this improvement by weighting each photon equally.

3.2 Description of Maximum-Likelihood Analaysis

The field of γ-ray astrophysics has generally found maximum-likelihood to be a dependable method to avoid the issues discussed above. The term likelihood was first introduced by Fisher (1925). Maximum-likelihood was applied to photon-counting experiments in the context of astrophysics by Cash (1979). Mattox et al. (1996) described the maximum-likelihood analysis framework devoped to analyze EGRET data.

In the formulation, one relies upon primarily upon the likelihood function. The likelihood, denoted $\mathcal{L}$, is quite simply the probability of obtaining the observed data given an assumed model:

$$\mathcal{L} = P(\text{data}|\text{model}) \tag{3.1}$$

Section 3.3 will provide describe the components that go into a model of the data.

Generaly, a model of the sky depends upon a list of parameters that we denote as $\vec{\lambda}$. Therefore, the likelihood function itself becomes a function of the parameters of the model:

$$\mathcal{L} = \mathcal{L}(\vec{\lambda}) \tag{3.2}$$

The term maximum-likelihood refers to the fact that the best-fit parameters of a model can be estimated by maximizing the likelihood function.

What are the benefits of maximum likelihood

Describe Wilk's Therorem and it's application to parameter error estimation

3.3 Defining a Model of the Sources in the Sky

In order to perform a maximum-likelihood analysis, one requires a parameterized model of the sky. A model of the sky is composed of a set of γ-ray sources, each

characterized by its photon flux density $\mathcal{F}(E, t, \vec{\Omega}|\vec{\lambda})$. This represents the number of photons emitted per unit energy, per unit time, per units solid angle at a given energy, time, and position in the sky. In The Centimetre-Gram-Second System of Units (CGS), it has units of ph $\mathrm{cm}^{-2}\mathrm{s}^{-1}\mathrm{erg}^{-1}\mathrm{sr}^{-1}$.

Often, the spatial and spectral part of the source model are separable and independent of time. When that is the case, we like to write the source model as

$$\mathcal{F}(E, t, \vec{\Omega}|\vec{\lambda}) = \frac{dN}{dE} \times \mathrm{PDF}(\vec{\Omega}). \tag{3.3}$$

Here, $\frac{dN}{dE}$ is only a function of energy and PDF $(\vec{\Omega})$ is only a function of position $(\vec{\Omega})$. In this formulation, some of the model parameters $\vec{\lambda}$ are taken by the $\frac{dN}{dE}$ function and some by the PDF$(\vec{\Omega})$ function. In CGS, $\frac{dN}{dE}$ is in units of ph $\mathrm{cm}^{-2}\mathrm{s}^{-1}\mathrm{erg}^{-1}$.

The spectrum $\frac{dN}{dE}$ is typically modeled by simple geometric functions. The most popular spectral model is a power law (PL):

$$\frac{dN}{dE} = N_0 \left(\frac{E}{E_0}\right)^{-\gamma} \tag{3.4}$$

Here, $\frac{dN}{dE}$ is a function of energy and also fo the two model parameters (the prefactor N_0 and the spectral index γ). The parameter E_0 is often called the energy scale or the pivot energy and is not considered a model parameter.

Another common spectral model is the broken-power law (BPL) spectral model

$$\frac{dN}{dE} = N_0 \times \begin{cases} (E/E_b)^{-\gamma_1} & \text{if } E < E_b \\ (E/E_b)^{-\gamma_2} & \text{if } E \geq E_b \end{cases} \tag{3.5}$$

This model represents a powerlaw with an index of γ_1 which has a break at energy E_b to having an index of γ_2.

Finally, the exponentially-cutoff power law (ECPL) spectral model is often used to model the γ-ray emission from pulsars:

$$\frac{dN}{dE} = N_0 \left(\frac{E}{E_0}\right)^{-\gamma} \exp\left(-\frac{E}{E_c}\right). \tag{3.6}$$

For energies much below E_c, the ECPL is a PL with spectral index γ. For energies much larger than E_c, the ECPL exponentially decreases.

PDF represents the spatial distribution of the emisison. It is traditionally normalized as though it was a probability:

$$\int d\Omega \, \mathrm{PDF}(\vec{\Omega}). \tag{3.7}$$

Therefore, in CGS PDF has units of sr^{-1} For a point-like source at a position $\vec{\Omega}'$, the spatial model is:

$$\mathrm{PDF}(\vec{\Omega}) = \delta(\vec{\Omega} - \vec{\Omega}') \tag{3.8}$$

and is a function of the position of the source. Example spatial models for spatially-extended sources will be presented in section XXXXX

This formulation assumed that the source models are not time dependent. This is traditionally because it is difficult to find simple paremterized models to fit the time behavior of a variable source. Instead, the typtical strategy to fit varaible sources is to divide a large range of time into multiple smaller time intervals and to perform multiple likelihood fits in each time range.

In some situations, the spatial and spectral part of a source do not nicely decouple. An example of this could be **SNR!**s (**SNR!**s) which could show a spectral variation across the source. Katsuta et al. (2012) and Hewitt et al. (2012) have simplied this problem by A simple method which has been adopted to study this kind of sourcc.

FINISH DISCUSSION

In situations where spatial and spectral components couple, typical to make multiple spatial templates, each with an indepdnet spectra (e.g. the Puppis A paper's fitting multiple hemispheres).

Discuss how diffuse background is more complciated and requires a mapcube.

WHAT SECTION DESCRIBES EXTENDED SOURCE PDFs

3.4 The LAT Instrument Response Functions

The performance of the LAT is composted of two effects. The efficiency of the LAT referes to its ability to to reconstruct a photon which comes into the detect. The disperson of the LAT refers to the probability of misreconstructing an event.

The efficiency is typically called the effective area. We write it as $\epsilon(E, t, \vec{\Omega})$. It is a function of energy, time, and Solid Angle (SA). It is measured in units of area (cm^2).

LINK TO arXiv:1206.1896 for MORE THOUROUGH DISCUSSION OF EFFECTIVE AREA

DISCUSS HOW EFFECTIVE AREA IS A FUNCTION OF DIFFERENT THINGS

The dispersion is the probability of a photon with true energy E and incoming direction $\vec{\Omega}$ at time t being reconstructed to to have an energy E', an incomming direction $\vec{\Omega}'$ at a time t'. The dispersion is written as $P(E', t', \vec{\Omega}'|E, t, \vec{\Omega})$. It represents a probability and is therefore normalized such that

$$\int\int\int dE d\Omega dt P(E', t', \vec{\Omega}'|E, t, \vec{\Omega}) = 1 \tag{3.9}$$

What is the range of the integrals

Therefore, $P(E', t', \vec{\Omega}'|E, t, \vec{\Omega})$ has units of 1/energy/SA/time

We assume these two factors to decouple and write the LAT's instrument response as

$$R(E', \vec{\Omega}', t'|E, \vec{\Omega}, t) = \epsilon(E, t, \vec{\Omega}) P(E', t', \vec{\Omega}'|E, t, \vec{\Omega}) \tag{3.10}$$

Therefore, the instrument response has units of area/energy/SA/time

The convolution of the flux of a model with the instrument response produces the expected counts per unit energy/time/SA begin reconstructed to have an energy E' at a position $\vec{\Omega}'$ and at a time t':

$$\tau(E', \vec{\Omega}', t'|\vec{\lambda}) = \int\int\int dE\, d\Omega\, dt\, \mathcal{F}(E, t, \vec{\Omega}|\vec{\lambda}) R(E', \vec{\Omega}', t'|E, \vec{\Omega}, t) \tag{3.11}$$

Here, this integral is performed over all true energies, SAs, and times for which the source model has support.

For LAT analysis, we conventionally make the simplifying assumption that the energy , spatial , and time dispersion decouple:

$$P(E', t', \vec{\Omega}'|E, t, \vec{\Omega}) = \mathrm{PSF}(\vec{\Omega}'|E, \vec{\Omega}) \times \mathrm{E_{disp}}(E'|E) \times \mathrm{T_{disp}}(t'|t) \tag{3.12}$$

Here, PSF is the point-spread function and represents ...

BETTER DISCUSSION OF PSF OF THE LAT, WHAT ITS SCALE IS...

$\mathrm{E_{disp}}$ represents the energy dispersion of the LAT. The energy dispersion of the LAT is a function of both the incident energy and incident angle of the photon. It varies from $\sim$ 5% to 20%, degrading at lower energies due to energy losses in the tracker and at higher energy due to electromagnetic shower losses outside the calorimiter. Similarly, it improves for photons with higher incident angles that are allowed a longer path through the calorimieter (Ackermann et al. 2012).

For sources with smoothly-varying spectra, the effects of ignoring the inherent energy dispersion of the LAT are typically small. Ackermann et al. (2012) performed a monte carlo simulation to show that for power-law point-like sources, the bias introduced by ignoring energy dispersion was on the level of a few perect. Therefore, energy dispersion is typicially ignored for standard likelihood analysis:

$$\mathrm{E_{disp}} = \delta(E - E') \tag{3.13}$$

We cauation that for analysis of sources extended to energies below 100 MeV and for sources expected to have spectra that do not smoothly vary, the effects of energy dispersion could be more severe.

- $\mathrm{T_{disp}}$ is the time dispersion.
-
- The timing dispersion is < 10 μs Atwood et al. (2009)
- WRITE ENERGY DISPERSION AS A DELTA FUNCTION

Why discard time dispersion

Therefore, the instrument response is typically approximated as FINISH

$$R(E', \vec{\Omega}', t'|E, \vec{\Omega},) = \epsilon(E, t', \vec{\Omega})\mathrm{PSF}(\vec{\Omega}'|E, \vec{\Omega}) \tag{3.14}$$

The expected count rate is then typically integrated over time to compute the total counts. Assuming that the source model is time indepdendent, we get:

$$\tau(E', \vec{\Omega}'|\vec{\lambda}) = \int d\Omega\, \mathcal{F}(E, \vec{\Omega}|\vec{\lambda}) \left(\int dt\ \epsilon(E, t, \vec{\Omega}) \right) \mathrm{PSF}(\vec{\Omega}'|E, \vec{\Omega}) \tag{3.15}$$

This equation essentially says that the counts expected by the LAT for the particular model is the product of the source's flux with the effective area and then convolved with the point-spread function.

Figure out how the θ depedence of the IRFs factors into this calcualtion

3.5 Binned Maximum-Likelihood of LAT Data with the Science Tools

- For a standard LAT analysis, we perform a binned maximum-likelihood analysis:
- In the standard science tools, the data is binned in position and energy. and integrated in energy.
- For time-serires analysis, typically a time-summed analysyis is performed successivly in multiple time bins.
- The likelihood comes from a sum over each bin
- The likelihood is defined as

$$\mathcal{L} = \prod_j \frac{\theta_j^{n_j} e^{-\theta_j}}{n_j!} \tag{3.16}$$

  - Here, j is a sum over position/energy bins.

  - θ_j is the counts predicted by the model, which is defiend followign the discussion in Section 3.3.
  - n_j are the observed counts in the spatial/energy bin j

- The model counts are computed by integrating the differential counts defined in Equation 3.11 over the energy bin:

$$\theta_{ij} = \int_j dE\ d\Omega\ dt\ \tau(E, \vec{\Omega}, t|\vec{\lambda}_i) \tag{3.17}$$

  Here, j represents the integral over the jth position/energy bin, i represents the ith source, and $\vec{\lambda}_i$ refers to the parmeters defining the ith source. The total model counts is computed by summing over all sources:

$$\theta_j = \sum_i \theta_{ij} \tag{3.18}$$

- In the standard *Fermi* science tools, the binning of photons over position in the sky and energy to compute n_j is done with `gtbin`.
- In the standard *Fermi* science tools, the model counts θ_j are computed in several steps ...
- The instrument response is computed with a combination of `gtltcube`, `gtexpcube`.
- Convert a model of the sky into model predicted counts
- poisson likelihood
- Particular implemenation of maximum likelihood anlaysis
- Describe `gtbin`, `gtselect`, `gtlike`

Write Section or Perform simple MC Simulation to demonstrate signficance of detection

3.6 The Alternate Maximum-Likelihood Package `pointlike`

- Developed for Speed
- Sparce Matricies,
- Methods for computing integral model counts.

Chapter 4

Analysis of Spatially Extended LAT Sources

4.1 Analysis Method

4.2 Validation of the TS Distribution

4.3 Extended Source Detection Threshold

4.4 Testing Against Source Confusion

4.5 Test of 2LAC Sources

4.6 Systematic Errors on Extension

Chapter 5

Search for Spatially-extended Sources

5.1 Extended Source Search Method

5.2 New Extended Sources

5.3 Discussion

Chapter 6

Search for PWNe associated with Gamma-loud Pulsars

6.1 Off-peak Phase Selection

6.2 Off-peak Analysis Method

6.3 Off-peak Results

6.4 Off-Peak Individual Source Discussion

Chapter 7

Search for PWNe associated with TeV Pulsars

Notes

- Only include sources classified as PWN in TeVCat.
- Always model LAT Pulsar in the background (???)

7.1 List of Candidates

7.2 Analysis Method

7.3 Sources Detected

Chapter 8

Search for PWNe associated with High $\dot{E}$ Pulsars

Chapter 9

Population Study of LAT-detected PWNe

Bibliography

Ackermann, M., Ajello, M., Albert, A., et al. 2012, ApJS, 203, 4

Arnold, J. R., Metzger, A. E., Anderson, E. C., & van Dilla, M. A. 1962, J. Geophys. Res., 67, 4878

Atwood, W. B., Abdo, A. A., Ackermann, M., et al. 2009, ApJ, 697, 1071

Baum, W. A., Johnson, F. S., Oberly, J. J., et al. 1946, Phys. Rev., 70, 781

Bertsch, D. L., Brazier, K. T. S., Fichtel, C. E., et al. 1992, Nature, 357, 306

Bignami, G. F., Boella, G., Burger, J. J., et al. 1975, Space Science Instrumentation, 1, 245

Browning, R., Ramsden, D., & Wright, P. J. 1971, Nature Physical Science, 232, 99

Burnight, T. 1949, Phys. Rev, 76, 19

Cash, W. 1979, ApJ, 228, 939

Critchfield, C. L., Ney, E. P., & Oleksa, S. 1952, Physical Review, 85, 461

Feenberg, E., & Primakoff, H. 1948, Phys. Rev., 73, 449

Fichtel, C. E., Hartman, R. C., Kniffen, D. A., et al. 1975, ApJ, 198, 163

Fisher, R. A. 1925, Statistical Methods for Research Workers (Edinburgh: Oliver and Boyd)

Hayakawa, S. 1952, Progress of Theoretical Physics, 8, 571

Herschel, W. 1800, Philosophical Transactions of the Royal Society of London, 90, pp. 284

Hewitt, J., Grondin, M.-H., Lemoine-Goumard, M., et al. 2012

Hulsizer, R. I., & Rossi, B. 1948, Phys. Rev., 73, 1402

Hutchinson, G. 1952, Philosophical Magazine Series 7, 43, 847

Jansky, K. 1933, Proceedings of the Institute of Radio Engineers, 21, 1387

Katsuta, J., Uchiyama, Y., Tanaka, T., et al. 2012

Kerr, M. 2010, PhD thesis, University of Washington

Kniffen, D. A., & Fichtel, C. E. 1970, ApJ, 161, L157

Kraushaar, W., Clark, G. W., Garmire, G., et al. 1965, ApJ, 141, 845

Kraushaar, W. L., Clark, G. W., Garmire, G. P., et al. 1972, ApJ, 177, 341

Li, T.-P., & Ma, Y.-Q. 1983, ApJ, 272, 317

Mattox, J. R., Bertsch, D. L., Fichtel, C. E., et al. 1992, ApJ, 401, L23

Mattox, J. R., Bertsch, D. L., Chiang, J., et al. 1996, ApJ, 461, 396

Morrison, P. 1958, Il Nuovo Cimento, 7, 858

Nolan, P. L., Abdo, A. A., Ackermann, M., et al. 2012, ApJS, 199, 31

Rousseau, R., Grondin, M.-H., Van Etten, A., et al. 2012, A&A, 544, A3

Swanenburg, B. N., Hermsen, W., Bennett, K., et al. 1978, Nature, 275, 298

Swanenburg, B. N., Bennett, K., Bignami, G. F., et al. 1981, ApJ, 243, L69

Thompson, D. J., Fichtel, C. E., Hartman, R. C., Kniffen, D. A., & Lamb, R. C. 1977a, ApJ, 213, 252

Thompson, D. J., Fichtel, C. E., Kniffen, D. A., & Ogelman, H. B. 1977b, ApJ, 214, L17